High-resolution fMRI detects neuromodulation of individual brainstem nuclei by electrical tongue stimulation in balance-impaired individuals

Joseph C. Wildenberg[*,a,b], **Mitchell E. Tyler**[c,e], **Yuri P. Danilov**[c], **Kurt A. Kaczmarek**[c], and **Mary E. Meyerand**[a,d,e]

[a] Neuroscience Training Program, University of Wisconsin-Madison, Madison, WI 53705, USA

[b] Medical Scientist Training Program, University of Wisconsin-Madison, Madison, WI 53705, USA

[c] Department of Orthopedics and Rehabilitation, University of Wisconsin-Madison, Madison, WI 53705, US

[d] Department of Medical Physics, University of Wisconsin-Madison, Madison, WI 53705, USA

[e] Department of Biomedical Engineering, University of Wisconsin-Madison, Madison, WI 53706, USA

Abstract

High resolution functional magnetic resonance imaging (fMRI) can be used to precisely identify blood-oxygen-level dependent (BOLD) activation of small structures within the brainstem not accessible with standard fMRI. A previous study identified a region within the pons exhibiting sustained neuromodulation due to electrical tongue stimulation, but was unable to precisely identify the neuronal structure involved. For this study, high-resolution images of neural activity induced by optic flow were acquired in nine healthy controls and nine individuals with balance dysfunction before and after information-free tongue stimulation. Subjects viewed optic flow videos to activate the structures of interest. Sub-millimeter in-plane voxels of structures within the posterior fossa were acquired using a restricted field of view. Whole-brain functional imaging verified that global activation patterns due to optic flow were consistent with previous studies. Optic flow activated the visual association cortices, the vestibular nuclei, and the superior colliculus, as well as multiple regions within the cerebellum. The anterior cingulate cortex showed decreased activity after stimulation, while a region within the pons had increased post-stimulation activity. These observations suggest the pontine region is the trigeminal nucleus and that tongue stimulation interfaces with the balance-processing network within the pons. This high-resolution imaging allows detection of activity within individual brainstem nuclei not possible using standard resolution imaging.

* Corresponding Author: 1122o Wisconsin Institutes for Medical Research, 1111 Highland Ave., Madison, WI 53705, USA, jcwildenberg@wisc.edu, Phone: 1-608-695-0095, Fax: 1- 608-265-9840.

1. Introduction

Many separate neuronal structures must work together to collect and process environmental information pertinent to maintaining balance. These structures include components of the visual system, the vestibular nuclei and cerebellar flocculus/nodulus (the vestibular system), and the cerebellar hemispheres (proprioception and coordination). In addition, the parieto-insular vestibular cortex (PIVC) is a multi-modal processing center that integrates information from all of the involved sensory systems (Brandt and Dieterich 1999). Damage to any of these structures, regardless of the exact underlying etiology, can produce deficits of balance, posture, and gait. Unfortunately, few disorder-specific treatments exist and permanent disability is possible depending on the severity of the disease (Brandt et al., 2010).

One dominant effect of balance dysfunction is hypersensitivity to dynamic visual stimuli. Many individuals with balance disorders complain of increased sensitivity to significant motion within their visual field (Bronstein 2004) and the postural response to visual motion is one component of the sensory organization test (SOT) commonly used in the clinical assessment of individuals with balance dysfunction (Furman 1994; Mirka and Black 1990; Visser et al., 2008). Optic flow, a type of visual stimulus implying relative motion between the visual scene and the observer, can produce the sensation of egomotion. Optic flow can be used to measure the sensitivity of the visual system and the ability of the balance-processing network to integrate pertinent information (Kelly, Loomis, Beall 2005; O'Connor et al., 2008; Palmisano et al., 2009). This type of stimulus is especially useful in activating components of the balance-processing network when the subject is motionless, for example in investigations using functional magnetic resonance imaging (fMRI) (Cardin and Smith 2010; Kikuchi et al., 2009; Ohlendorf et al., 2008). Several previous studies have shown increased postural responses and hypersensitivity of the motion-sensitive visual cortices when balance-impaired individuals view optic flow (Dieterich et al., 2007; Mergner et al., 2005; Redfern and Furman 1994; Wildenberg et al., 2010).

Recent studies have shown that electrical stimulation of the tongue can produce behavioral improvements in many individuals who have some sensory impairment. This route to the brain was originally used for sensory substitution in both balance-impaired and blind individuals (Chebat et al., 2007; Danilov et al., 2006; Robinson et al., 2009; Tyler, Danilov, Bach-Y-Rita 2003; Vuillerme et al., 2008; Vuillerme and Cuisinier 2009). Cross-modal recruitment theories of plasticity can explain why individuals using the tongue stimulation for sensory substitution show improvement in behavioral tasks (Collignon et al., 2009; Pietrini, Ptito, Kupers 2009; Poirier, De Volder, Scheiber 2007; Ptito et al., 2005). One important observation of some balance studies was that the beneficial effects were sustained, lasting days to weeks beyond the final stimulation session (Danilov et al., 2006; Tyler, Danilov, Bach-Y-Rita 2003).

We recently demonstrated that such beneficial effects can be generated even when the stimulation signal contains no environmental information (Wildenberg et al., 2010). Information-free stimulation of the tongue, termed Cranial Nerve Non-Invasive Neuromodulation (CN-NINM), produced behavioral improvements that persisted after the stimulation electrodes were removed from the mouth. Imaging data collected in that study revealed that tongue stimulation causes sustained modulation in the processing of optic flow

within some neuronal structures involved in processing balance information. Of particular interest was modulation of a region within the pons of the brainstem. This region likely contains the vestibular, trigeminal, and solitary nuclei. The trigeminal nuclei receive somatosensory afferents from the tongue (cranial nerve five), while the solitary nuclei receive taste afferents from the chorda tympani nerve. Complex interactions between these structures (e.g. convergence and co-modulation of visual, vestibular, visceral sensory and nociceptive signals) may be involved in development and/or manifestation of various symptoms such as hypersensitivity to optical flow in balance and anxiety disorders, balance dysfunction in migraine disorders, and interoception (physiological sense of well-being) related homeostasic responses (Balaban and Thayer 2001; Buisseret-Delmas et al., 1999; Craig 2002; Jacob, Redfern, Furman 1995; Marano et al., 2005; Satoh, Ishizuka, Murakami 2009).

Our current hypothesis is that these structures and their interconnections are modulated by electrical stimulation applied to the tongue. Sustained changes in information processing within these structures could explain the behavioral and subjective improvements seen in previous studies using this technique.

The brainstem and cerebellum present many challenges for imaging. Not only are the neuronal structures within these regions much smaller than those within the cortex, but the posterior fossa is extremely susceptible to magnetic field inhomogenities and large motion artifacts as the brainstem moves with arterial pulsation and respiration. Additional field inhomogenities are produced by the brainstem's proximity to the oropharynx. Multiple techniques to correct for these artifacts are effective at increasing the blood-oxygen-level dependent (BOLD) contrast and SNR (Tracey and Iannetti 2006). Precise localization and attribution of activation to individual nuclei requires increased spatial resolution to counteract the partial-volume effects that result when the target structure is similar (or smaller) in size to the voxels being collected (Figure 1 A-C) (Weibull et al., 2008). Although very suggestive, the standard resolution fMRI used in our previous study could not distinguish between individual nuclei within the brainstem and it was not possible to identify which nuclei were modulated by the stimulation.

To precisely identify which brainstem and cerebellar structures are modulated by electrical tongue stimulation this study utilized high-resolution fMRI imaging to collect sub-millimeter axial voxels while individuals with balance-dysfunction and healthy controls viewed optic flow (Figure 1 D-F). The stimulation techniques used are identical to those from our previous study except that these subjects received an additional week of stimulation to strengthen potential sustained neuromodulation (Wildenberg et al., 2010).

2. Methods

To achieve sufficient statistical significance for inter-subject comparison, we used an a priori power analysis to estimate the appropriate number of study participants. Our previous study found mean BOLD signal changes within the brainstem of 0.2% with a standard deviation of approximately 0.1% using identical visual stimuli to the one used in this study (Wildenberg et al., 2010). These values give a standardized effect size of $(0.2/0.1)/2 = 1.0$. We choose an acceptable type-I error of $\alpha = 0.05$ and a power of $P = 1 - \beta = 0.80$. Using a power table for two-way ANOVAs calculated by Bausell and Yi, we find an estimated sample size of 9 participants per group (Bausell and Li 2002). This sample size also provides adequate power for intergroup comparisons using two-sample *t*-tests (Rosner 2006).

2.1 Subjects

Nine subjects identified by symptoms of chronic balance dysfunction (M/F: 2/7, mean age 47.0±11.5 years) and nine controls (M/F: 5/4, mean age 38.8±16.1 years) participated in this study. Balance-impaired subjects were recruited primarily through referral from clinicians aware of ongoing studies within our research group. These balance-impaired subjects were located throughout the United States and travelled to our facility for participation in the study. Controls were recruited from the general population around Madison, Wisconsin. Subject recruitment occurred from May 2009 through September 2010.

Inclusion criteria for the balance subjects were broad and included individuals with a chronic, stable balance dysfunction that affected balance, posture, and gait. Exclusion criteria, for both balance subjects and controls, were pregnancy, mental health disorders, corrected vision below 20/40, myasthenia gravis, Charcot-Marie-Tooth disease, post-polio syndrome, Guillan-Barré, fibromyalgia, chronic fatigue syndrome, herniated disc, and osteoarthritis of the spine. Exclusion criteria for balance-impaired subjects also included communicable diseases (HIV, TB, hepatitis, etc.), oral health problems (open sores in the mouth or tongue), and any neurological disorder not attributed to their primary diagnosis. Subjects were also excluded if they had MRI-incompatible metallic implants. The University of Wisconsin-Madison Health Sciences Institutional Review Board approved all aspects of this study and all subjects signed the approved consent form before beginning any portion of the study. Subjects completed consent, screening, and informational forms during their first visit. Subjects were not compensated for participation in this study.

2.2 Visual stimuli and display

Two visual stimuli were used to activate structures involved in balance processing while subjects remained stationary within the MRI scanner. The control stimulus (static) was a static checkerboard of alternating white and black squares with an edge length of 230 pixels. Two-dimensional optic flow (dynamic) was presented using a video derived from the static checkerboard image. An apparent in/out motion arose from varying the size of the squares using a sinusoidal oscillation with a frequency of 0.2 Hz. Additionally, rotation about the center of the viewfield was produced using the superposition of two sinusoids (0.2 and 0.35 Hz) to prevent prediction of the motion. These stimuli were identical to those described in our previous study (Wildenberg et al., 2010). Both stimuli had a total image size of 800×600 pixels (equal to the resolution of the display goggles) and the dynamic video was displayed at 60 frames-per-second.

During the functional MRI scans, all subjects were shown the two visual stimuli in a pseudo-randomized block-design paradigm. Each stimulus was displayed for twelve seconds in blocks of three to six repetitions. Within a block, the stimulus presentations were separated by six seconds of fixation to reduce the contamination of neural responses from one stimulus presentation into the next (O'Connor et al., 2008). Each block was also separated by six seconds of fixation. The order of stimulus presentation was the same for all subjects.

Subjects viewed the visual stimuli on MRI-compatible head-mounted display goggles (Resonance Technology, Northridge, CA). These goggles produce an 800×600 pixel display with a 30° horizontal and 22° vertical field-of-view in each eye. A mask of black fabric was placed over the subject's head and goggles to block all remaining ambient light.

2.3 MRI data collection

MRI data was acquired with a 3T MRI scanner (GE750, GE Healthcare, Waukesha, WI). T1-weighted anatomical images were collected using a spoiled gradient recalled pulse

sequence. A standard-resolution functional scan (stan-res) was acquired with a T2*-weighted gradient-echo echo-planar imaging (GE-EPI) sequence (TR = 2000 ms, echo time = 30 ms, flip angle = 75 degrees) to acquire BOLD signal over a 64×64 matrix and 42 axial slices (3.12 × 3.12 × 3.2 mm resolution). An additional high-resolution functional scan (high-res) was acquired using the same imaging parameters, but with a 256×256 matrix and 23 axial slices (0.86 × 0.86 × 2.9 mm resolution) covering only the posterior fossa. The order of the scans was randomized to eliminate the effect of inter-scan habituation to the visual stimuli. The first four volumes of each functional scan (152 total volumes) were automatically discarded to allow the longitudinal magnetization to reach equilibrium. Cardiac and respiratory waveforms were collected during the functional scans for use in physiologic artifact removal during data analysis.

2.4 Behavioral testing

The nine balance-impaired subjects completed sensory organization testing (NeuroCom International, Clackamas OR, USA) at the University of Wisconsin Sports Medicine facility to measure dynamic behavioral impairment (Furman 1994). The test gives a composite score that combines performance on six sensory conditions and is a measure of overall postural stability. A composite score below 70 is defined as outside the normal range.

2.5 Tongue stimulation

Stimulation to the tongue was delivered via a small electrode array placed on the anterior portion of the tongue and held in place by pressure of the tongue to the roof of the mouth (Tyler, Danilov, Bach-Y-Rita 2003). The sensation produced by the array is similar to drinking a carbonated beverage.

CN-NINM stimulation consists of three square-pulse bursts delivered equally to all electrodes with an intraburst frequency of 200Hz and an interburst frequency of 50 Hz that does not vary throughout the duration of the stimulation session. Previous studies had coupled the array to a helmet-mounted accelerometer to give feedback on the direction of gravity (Danilov et al., 2007; Danilov et al., 2006; Vuillerme and Cuisinier 2009). In this study, the signal was not coupled to any sensor and did not provide any useful environmental information to the subject.

2.6 Procedure

On the day of the first visit (day 0), all subjects underwent an fMRI scan to collect neural responses to the visual stimuli. No tongue stimulation was given during the fMRI scans. Balance-impaired subjects also performed sensory organization testing (SOT). Data from this session will be referred to as Pre (balance-impaired subjects) or Nor (normal controls).

CN-NINM stimulation was delivered only to the balance-impaired subjects over 19 stimulation sessions (two on days 1-9 and one on day 10). Days 5 and 6 were separated by two rest days in which the subjects did not receive any stimulation. During a stimulation session, subjects received continuous stimulation for 20 minutes, wherein the subject stood as still as possible with their feet together and eyes closed. A physical therapist was always present to prevent falls.

After completion of the nineteen stimulation sessions, balance-impaired subjects repeated the fMRI scans and SOT testing. The procedures for the tests on day 10 were identical to those completed on day 0. This data from balance-impaired subjects (Post) were collected between three and six hours after the final stimulation session.

2.7 MRI data analysis

fMRI data was preprocessed using the AFNI software suite (Cox 1996). This included corrections for slice-time acquisition errors and subject motion, temporal low-pass filtering with a 0.15 Hz cutoff, and spatial smoothing. The stan-res data was smoothed using an isotropic Gaussian filter having a full width at half maximum (FWHM) of 8mm. The high-res data was smoothed with a 3mm filter. For input to the general linear model (GLM), the task waveforms were combined to look at the effect of any visual stimulus (Photic: static and dynamic) and the effect of visual motion (Motion: dynamic only). The GLM was estimated with the SPM8 software package and included regressors for subject motion and physiologic parameters (Johnstone et al., 2006; Lund et al., 2005). Respiratory and cardiac waveforms collected during the functional scans were processed using a script by Kelley *et al.* prior to inclusion in the GLM (Kelley et al., 2008). GLM output was converted to percent signal change by dividing each contrast image by the baseline image.

The stan-res data was normalized using the SPM8 algorithm. Normalization of the high-res data was performed using the SUIT algorithm and atlas plugin for SPM8 as this more accurately aligns the brainstem and cerebellum than whole-brain normalization (Diedrichsen 2006; Diedrichsen et al., 2009). The data was resampled to a resolution of $2\times2\times2$ mm^3 (stan-res) or $1\times1\times2$ mm^3 (high-res) using 7th-degree b-splines, the most accurate resampling option available in SPM8.

Comparison of the balance-impaired subjects before and after stimulation was performed using a two-way repeated-measures ANOVA (separate for the stan-res and high-res data). The independent variables were the effects of optic flow (OF: Photic, Motion) and any sustained neuromodulation due to the stimulation (Stim: Pre, Post). OF data show activation attributable to visual motion by identify regions that have different activity during the dynamic stimulus compared to the static stimulus. Results for the factor Stim do not represent activation directly, but instead show regions whose activation pattern changed after the week of tongue stimulation (independent of the activations due to OF). Finally, the two-way interaction term OF × Stim reports brain regions that have altered activity when processing visual motion after stimulation compared to before. The displayed images and tables were created using *t*-tests to identify the directionality of the effect at each voxel.

As our study was unbalanced with respect to our two subject populations, the study design required group activation maps and intergroup comparisons to be performed using one- and two-sample *t*-tests. The one-sample tests show activation patterns due to optic flow in each group separately. The two-sample tests determine if these patterns are different between groups. Tests were performed separately for the stand-res and high-res data.

Corrections for multiple comparisons was performed using AFNI's *AlphaSim* Monte-Carlo simulations (Forman et al., 1995). This method allows for a combination of thresholding and spatial clustering to derive a corrected *p*-value. Results from these simulations indicated that only activation clusters at the $\alpha \leq 0.005$ threshold with a volume greater than 1144 μl (stand-res) or 40 μl (high-res) would have global significance at $p \leq 0.05$. While these volumes are acceptable for cortical structures, 40 μl is larger than most brainstem nuclei (Alvarez et al., 2000). Therefore, the minimum volume cutoff for the high-res clusters was 20 μl. Only clusters with volumes greater than these cutoffs are displayed in the figures and tables.

3. Results

3.1 Behavioral results

Balance-impaired subject 3 did not receive a score on the pre-stimulation SOT due to significant stability impairment and was omitted from the behavioral analysis. Subject 3

received a composite score of 62 on the post-stimulation test. Six of the remaining eight subjects had impaired performance, defined as having initial SOT composite scores below 70 (Figure 2). After CN-NINM stimulation, two subjects remained below this level. The average improvement in SOT scores was 15.75 with a standard error of the mean of 5.59 (p = 0.026, paired student's t-test).

3.2 Stan-res data

ANOVA suggests optic flow-related activations (OF) of multiple visual association cortices including hMT+/V5 and V3A (Table 1, Figure 3). No significant activation differences were attributable to the week of CN-NINM stimulation alone (Stim). There was one area of decreased optic flow-related activation after CN-NINM (OF × Stim). This cluster is in the middle of the anterior cingulate cortex bilaterally.

One- and two-sample t-tests showed each group had similar optic flow-induced activation patterns including the lateral occipital gyrus and superior parietal lobule (Table 2, Figure 4). In addition, control individuals showed a strong bilateral activation of the superior colliculus. Both before and after stimulation balance subjects showed lower optic flow-related activity of the occipital poles bilaterally compared to controls.

3.3 High-res data

Optic flow activated the right superior colliculus, the right vestibular nucleus, and multiple cerebellar structures (Table 3, Figure 5). A comparison of these activation patterns before and after CN-NINM stimulation (OF × Stim) revealed increased activation of a structure within the pons, which appears to be the trigeminal nucleus, and several increases and decreases within the cerebellum. Again, there were no significant clusters for the effect of stimulation alone.

The Pre and Post one-sample t-tests did not produce many areas of optic flow-induced activation (Table 4). Normal controls (Nor) had activation of several regions including the superior colliculus and many regions throughout the cerebellum. There were no significant differences between controls and balance subjects before stimulation. Balance subjects after stimulation had decreased optic flow-related activity of the nodulus and increased activity within the superior semilunar lobe of the cerebellum.

4. Discussion

Six of the eight balance-impaired subjects had improved SOT composite scores after CN-NINM stimulation. These improvements are consistent with the results of our previous study which used additional measures of balance and stability. As no stimulation was provided during these behavioral tests, any improvement is presumably due to the sustained effects of CN-NINM.

In the reported results for the stan-res and high-res data, there are occasionally statistical clusters that appear in the ANOVA analysis, but are not in the one-sample t-tests of the balance subjects. Two possibilities could explain why activation is seen in one analysis and not the other. First, the ANOVA analysis includes three explanatory factors in the model: activity attributable to optic flow (OF), activity attributable to the sustained effects of the stimulation (Stim), and an interaction term including both of those effects (OF × Stim). The t-tests only include a term for activity due to optic flow. This allows the ANOVA to be more sensitive in detecting lower-magnitude activation. Second, in the ANOVA analysis all data from both Pre and Post are analyzed together. This allows for increased power in detecting activity patterns due to optic flow. In the t-tests, each group is analyzed separately and therefore has less power.

The activation pattern due to optic flow is very similar to that seen in our previous study using a similar subject population and identical visual stimuli (Wildenberg et al., 2010). Activated cortical structures include V5/ hMT+ and V3A as well as the cingulate sulcus visual area (CSv). These activations are consistent with many previous studies investigating optic flow using fMRI (Cardin and Smith 2010; Cardin and Smith 2010; Indovina et al., 2005; Kikuchi et al., 2009; Ohlendorf et al., 2008; Slobounov et al., 2006). Two previous studies suggested that V5/hMT+ is hypersensitive to visual motion in individuals with balance dysfunction (Dieterich et al., 2007; Wildenberg et al., 2010). Although we did not see significant differences between balance-impaired individuals and controls in this study, our data suggest that a larger sample size may have reproduced this result.

The high-resolution scans provided a much more precise view of the activations occurring within the brainstem and cerebellum. Optic flow activated multiple structures involved in processing visual motion information including the right vestibular nucleus and the right superior colliculus (Tables 3 and 4, and Figure 5). Multiple cerebellar structures were also activated, again consistent with activations seen in other fMRI studies utilizing optic flow.

There were no activity differences due to the sustained effects of CN-NINM stimulation (Stim). No clusters reached significance from either the high-res data or the stan-res data. These findings are consistent with our overall hypothesis that CN-NINM modulates activity within the balance-processing network, but only when it is actively processing pertinent sensory information. Without being activated by optic flow, there were no overall activity differences between the Pre and Post scans.

There were, however, several regions in the balance subjects that showed differences in optic-flow related activity after CN-NINM stimulation (OF × Stim). Within the cortex, the anterior cingulate area showed decreased optic flow-related activity after the week of stimulation. Additionally, a structure within the pons that appears to be the right trigeminal nucleus had an increased response to optic flow after CN-NINM. This is the site at which stimulation from the tongue enters the central nervous system (CNS) and may be the site of origin for the neuromodulation leading to improvement in behavioral and subjective measures. This result supports our hypothesis that the neuromodulation induced by CN-NINM is task dependent.

The anterior cingulate cortex (ACC) is involved in internal error monitoring and processing, violations of expectancy, and the resolution of discordant cognitive signals (Carter and van Veen 2007; Holroyd et al., 2004; Oliveira, McDonald, Goodman 2007). For example, Danckert and colleagues found increased activation of the ACC when healthy subjects were asked to point while wearing prism glasses, leading to errors between their visual and motor systems (Danckert, Ferber, Goodale 2008). Several other imaging studies using direct vestibular stimulation (caloric and galvanic) and visual stimulation have shown activations of the ACC (Calhoun et al., 2001; Kisely et al., 2002; Miyamoto et al., 2007). We believe the decreased activation of this region after CN-NINM represents the decreased ability of motion in the visual field to induce the sensation of ego-motion and therefore a reduction in the error signal processed by the ACC. This is likely due to a re-weighting of sensory inputs to the balance-processing network (Fetsch et al., 2009; Mahboobin et al., 2005).

The complexity of the cerebellum's functional structure and the intrinsic involvement of cerebellar networks in movement control and behavior make modulations of cerebellar structures more difficult to interpret. Other than the vermis and nodulus, which are involved in processing balance-pertinent stimuli, the exact contributions of many cerebellar nuclei to balance processing are still unknown (Angelaki et al., 2010). Ptito and colleagues found increased stimulation-induced cerebellar activation in blind individuals using PET (Matteau

et al., 2010; Ptito et al., 2005). The different subject populations and tasks prevent a direct comparison of these activations.

Finally, several studies using various techniques have found connections between the trigeminal nuclei and some components of the balance-processing network. For example, direct bi-directional connections with the vestibular nuclei may facilitate information transfer between these adjacent structures (Anker et al., 2003; Buisseret-Delmas et al., 1999; Herrick and Keifer 2000; Marano et al., 2005; Satoh, Ishizuka, Murakami 2009). Fujino *et al.* have found behavioral evidence for these connections in a study showing improved postural stability when subjects clenched their teeth, a movement requiring activation of the motor trigeminal system (Fujino, Takahashi, Ueno 2010). It is known that visual and vestibular information converge within the inferior olive and project to the vestibular nuclei (Barmack 2006; Gerrits, Voogd, Magras 1985). We believe CN-NINM stimulation may strengthen connections between the trigeminal and vestibular nuclei and sensitize the trigeminal nuclei to information present within the vestibular system. The increased response of the trigeminal nuclei to optic flow after stimulation may reflect this increased information transfer from the vestibular nuclei, a pathway not utilized in either balance-impaired subjects before stimulation nor healthy individuals (Figure 5). Recent studies, some using a similar tongue stimulation device, have also shown information transfer between the tongue and hMT+/V5 without using the normal visual-processing pathways, presumably directly through the thalamus. (Bicchi et al., 2008; Fries 1990; Matteau et al., 2010; Ricciardi et al., 2007; Wall, Symonds, Kaas 1982).

The ability for information-free tongue stimulation to produce sustained improvements in objective and subjective measures of balance is unexpected in the context of recruitment theories of plasticity (Collignon et al., 2009; Ptito et al., 2005). The results presented here hint at the potential for electrical stimulation to activate alternate pathways of information transfer not normally utilized – in this case between the balance-processing and trigeminal systems. We postulate that the cortical changes are the result of visual-motion information, now present in the trigeminal nuclei, propagating to the motion-sensitive visual cortices (Matteau et al., 2010). An alternate information pathway could partially explain the behavioral improvements and decrease in perceived discomfort due to visual motion after CN-NINM stimulation (Wildenberg et al., 2010). We emphasize that the fMRI measurements were performed without concurrent tongue stimulation. Any altered behavioral or fMRI measurements must therefore be the result of sustained neuroplastic changes due to CN-NINM.

One potential source of error stemmed from the heterogeneity of our balance-impaired subjects. Although responses to direct vestibular stimulation differ between central and peripheral vestibular disorders, responses to optic flow, which use the visual system instead of the vestibular system as input, seems to be similar regardless of the underlying etiology (Dieterich et al., 2007; Dieterich and Brandt 2008; Wildenberg et al., 2010). It is also possible that the stimulation sessions taught subjects to clench their tongues to the roof of their mouth when performing balance tasks. Such clenching has been shown to improve postural performance in healthy controls (Fujino, Takahashi, Ueno 2010). While some of the improvements seen on the behavioral tests could be due to this effect, we do not believe this explains the altered neural responses to optic flow as there was no exposure to optic flow during the stimulation sessions.

This study was limited by the lack of a sham stimulation subject group. The noticeable sensation of electrical stimulation of the tongue makes development of a realistic sham paradigm difficult. The intense visitation requirements would make recruitment of subjects

willing to be randomized to sham stimulation difficult, and a crossover study design was not appropriate for a pilot study.

5. Conclusion

This study utilized high-resolution imaging of the brainstem and cerebellum to precisely localize sustained subcortical neuromodulation induced by CN-NINM. A previous study showed that an area within the pons had a different response to optic flow after stimulation but was not able to identify the structure due to the small sizes of the nuclei within the brainstem (Wildenberg et al., 2010). The results of this study suggest that this region is likely the trigeminal nucleus, the point at which tongue stimulation enters the CNS. Anatomical connections and functional interactions between the adjacent vestibular and trigeminal nuclei may be strengthened by the stimulation, allowing visual-motion information present in the vestibular nuclei to activate the trigeminal. This alternate pathway for communication between the visual and vestibular system could partially explain the measured improvements in postural stability. Future studies that investigate the route by which brainstem and cerebellar neuromodulation propagates to the cortex are needed to understand how local subcortical changes can yield cortical activity changes and positive behavioral effects. The ability to non-invasively produce sustained modulation of neural activity holds promise as a new route for therapy in individuals with neurological dysfunction.

Acknowledgments

References

Alvarez JC, Diaz C, Suarez C, Fernandez JA, Gonzalez del Rey C, Navarro A, Tolivia J. Aging and the human vestibular nuclei: Morphometric analysis. Mechanisms of Ageing and Development. 2000; 114(3):149–172. [PubMed: 10802120]

Angelaki DE, Yakusheva TA, Green AM, Dickman JD, Blazquez PM. Computation of egomotion in the macaque cerebellar vermis. Cerebellum (London, England). 2010; 9(2):174–182.

Anker AR, Ali A, Arendt HE, Cass SP, Cotter LA, Jian BJ, Tamrazi B, Yates BJ. Use of electrical vestibular stimulation to alter genioglossal muscle activity in awake cats. Journal of Vestibular Research. 2003; 13(1):1–8. [PubMed: 14646019]

Balaban CD, Thayer JF. Neurological bases for balance-anxiety links. Journal of Anxiety Disorders. 2001; 15(1-2):53–79. [PubMed: 11388358]

Barmack NH. Inferior olive and oculomotor system. Progress in Brain Research. 2006; 151:269–291. [PubMed: 16221592]

Bausell, RB.; Li, Y. Power analysis for experimental research: A practical guide for the biological, medical and social sciences. Cambridge University Press; New York: 2002.

Bicchi A, Scilingo EP, Ricciardi E, Pietrini P. Tactile flow explains haptic counterparts of common visual illusions. Brain Research Bulletin. 2008; 75(6):737–741. [PubMed: 18394519]

Brandt T, Dieterich M. The vestibular cortex: Its locations, functions, and disorders. Annals of the New York Academy of Sciences. 1999; 871(1 OTOLITH FUNCTION IN SPATIAL ORIENTATION AND MOVEMENT):293–312. [PubMed: 10372080]

Brandt T, Huppert T, Hufner K, Zingler VC, Dieterich M, Strupp M. Long-term course and relapses of vestibular and balance disorders. Restorative Neurology and Neuroscience. 2010; 28(1):69–82. [PubMed: 20086284]

Bronstein AM. Vision and vertigo: Some visual aspects of vestibular disorders. Journal of Neurology. 2004; 251(4):381–387. [PubMed: 15083281]

Buisseret-Delmas C, Compoint C, Delfini C, Buisseret P. Organisation of reciprocal connections between trigeminal and vestibular nuclei in the rat. The Journal of Comparative Neurology. 1999; 409(1):153–168. [PubMed: 10363717]

Calhoun VD, Adali T, McGinty VB, Pekar JJ, Watson TD, Pearlson GD. fMRI activation in a visual-perception task: Network of areas detected using the general linear model and independent components analysis. NeuroImage. 2001; 14(5):1080–1088. [PubMed: 11697939]

Cardin V, Smith AT. Sensitivity of human visual and vestibular cortical regions to egomotion-compatible visual stimulation. Cerebral Cortex. 2010; 20(8):1964–1973. [PubMed: 20034998]

Carter CS, van Veen V. Anterior cingulate cortex and conflict detection: An update of theory and data. Cognitive, Affective & Behavioral Neuroscience. 2007; 7(4):367–379.

Chebat DR, Rainville C, Kupers R, Ptito M. Tactile-'visual' acuity of the tongue in early blind individuals. Neuroreport. 2007; 18(18):1901–1904. [PubMed: 18007183]

Collignon O, Voss P, Lassonde M, Lepore F. Cross-modal plasticity for the spatial processing of sounds in visually deprived subjects. Experimental Brain Research. 2009; 192(3):343–358.

Cox RW. AFNI: Software for analysis and visualization of functional magnetic resonance neuroimages. Computers and Biomedical Research. 1996; 29(3):162–173. [PubMed: 8812068]

Craig AD. How do you feel? interoception: The sense of the physiological condition of the body. Nature Reviews Neuroscience. 2002; 3(8):655–666.

Danckert J, Ferber S, Goodale MA. Direct effects of prismatic lenses on visuomotor control: An event-related functional MRI study. European Journal of Neuroscience. 2008; 28(8):1696–1704. [PubMed: 18973586]

Danilov Y, Tyler M, Skinner K, Hogle R, Bach-y-Rita P. Efficacy of electrotactile vestibular substitution in patients with peripheral and central vestibular loss. Journal of Vestibular Research. 2007; 17(2):119–130. [PubMed: 18413905]

Danilov, YP.; Tyler, ME.; Skinner, KL.; Bach-y-Rita, P. Efficacy of electrotactile vestibular substitution in patients with bilateral vestibular and central balance loss. Conference Proceedings : …Annual International Conference of the IEEE Engineering in Medicine and Biology Society.IEEE Engineering in Medicine and Biology Society; 2006. p. 6605-6609.

Diedrichsen J. A spatially unbiased atlas template of the human cerebellum. NeuroImage. 2006; 33(1): 127–138. [PubMed: 16904911]

Diedrichsen J, Balsters JH, Flavell J, Cussans E, Ramnani N. A probabilistic MR atlas of the human cerebellum. NeuroImage. 2009; 46(1):39–46. [PubMed: 19457380]

Dieterich M, Bauermann T, Best C, Stoeter P, Schlindwein P. Evidence for cortical visual substitution of chronic bilateral vestibular failure (an fMRI study). Brain. 2007; 130(8):2108–2116. [PubMed: 17575279]

Dieterich M, Brandt T. Functional brain imaging of peripheral and central vestibular disorders. Brain : A Journal of Neurology. 2008; 131(Pt 10):2538–2552. [PubMed: 18515323]

Duvernoy, HM. The human brain stem and cerebellum. Springer-Verlag; New York: 1995.

Fetsch CR, Turner AH, DeAngelis GC, Angelaki DE. Dynamic reweighting of visual and vestibular cues during self-motion perception. Journal of Neuroscience. 2009; 29(49):15601. [PubMed: 20007484]

Forman SD, Cohen JD, Fitzgerald M, Eddy WF, Mintun MA, Noll DC. Improved assessment of significant activation in functional magnetic resonance imaging (fMRI): Use of a cluster-size threshold. Magnetic Resonance in Medicine. 1995; 33(5):636–647. [PubMed: 7596267]

Fries W. Pontine projection from striate and prestriate visual cortex in the macaque monkey: An anterograde study. Visual Neuroscience. 1990; 4(3):205–216. [PubMed: 2078502]

Fujino S, Takahashi T, Ueno T. Influence of voluntary teeth clenching on the stabilization of postural stance disturbed by electrical stimulation of unilateral lower limb. Gait & Posture. 2010; 31(1): 122–125. [PubMed: 19879763]

Furman JM. Posturography: Uses and limitations. Bailliere's Clinical Neurology. 1994; 3(3):501–513.

Gerrits NM, Voogd J, Magras IN. Vestibular afferents of the inferior olive and the vestibulo-olivo-cerebellar climbing fiber pathway to the flocculus in the cat. Brain Research. 1985; 332(2):325–336. [PubMed: 3995273]

Herrick JL, Keifer J. Central trigeminal and posterior eighth nerve projections in the turtle< i> chrysemys picta</i> studied in vitro. Brain, Behavior and Evolution. 2000; 51(4):183–201.

Holroyd CB, Nieuwenhuis S, Yeung N, Nystrom L, Mars RB, Coles MGH, Cohen JD. Dorsal anterior cingulate cortex shows fMRI response to internal and external error signals. Nature Neuroscience. 2004; 7:497–498.

Indovina I, Maffei V, Bosco G, Zago M, Macaluso E, Lacquaniti F. Representation of visual gravitational motion in the human vestibular cortex. Science. 2005; 308(5720):416–419. [PubMed: 15831760]

Jacob RG, Redfern MS, Furman JM. Optic flow-induced sway in anxiety disorders associated with space and motion discomfort. Journal of Anxiety Disorders. 1995; 9(5):411–425.

Johnstone T, Ores Walsh KS, Greischar LL, Alexander AL, Fox AS, Davidson RJ, Oakes TR. Motion correction and the use of motion covariates in multiple-subject fMRI analysis. Human Brain Mapping. 2006; 27(10):779–788. [PubMed: 16456818]

Kelley DJ, Oakes TR, Greischar LL, Chung MK, Ollinger JM, Greene E. Automatic physiological waveform processing for fMRI noise correction and analysis. PLoS ONE. 2008; 3(3):e1751. [PubMed: 18347739]

Kelly JW, Loomis JM, Beall AC. The importance of perceived relative motion in the control of posture. Experimental Brain Research.Experimentelle Hirnforschung.Experimentation Cerebrale. 2005; 161(3):285–292. [PubMed: 15502985]

Kikuchi M, Naito Y, Senda M, Okada T, Shinohara S, Fujiwara K, Hori SY, Tona Y, Yamazaki H. Cortical activation during optokinetic stimulation - an fMRI study. Acta Oto-Laryngologica. 2009; 129(4):440–443. [PubMed: 19116795]

Kisely M, Emri M, Lengyel Z, Kalvin B, Horvath G, Tron L, Miko L, Sziklai I, Toth A. Changes in brain activation caused by caloric stimulation in the case of cochleovestibular denervation-PET study. Nuclear Medicine Communications. 2002; 23(10):967–973. [PubMed: 12352595]

Lund TE, Nørgaard MD, Rostrup E, Rowe JB, Paulson OB. Motion or activity: Their role in intra-and inter-subject variation in fMRI. NeuroImage. 2005; 26(3):960–964. [PubMed: 15955506]

Mahboobin A, Loughlin PJ, Redfern MS, Sparto PJ. Sensory re-weighting in human postural control during moving-scene perturbations. Experimental Brain Research Experimentelle Hirnforschung Experimentation Cerebrale. 2005; 167(2):260–267. [PubMed: 16025292]

Marano E, Marcelli V, Stasio ED, Bonuso S, Vacca G, Manganelli F, Marciano E, Perretti A. Trigeminal stimulation elicits a peripheral vestibular imbalance in migraine patients. Headache the Journal of Head and Face Pain. 2005; 45(4):325–331.

Matteau I, Kupers R, Ricciardi E, Pietrini P, Ptito M. Beyond visual, aural and haptic movement perception: HMT+ is activated by electrotactile motion stimulation of the tongue in sighted and in congenitally blind individuals. Brain Research Bulletin. 2010; 82:264–270. [PubMed: 20466041]

Mergner T, Schweigart G, Maurer C, Blümle A. Human postural responses to motion of real and virtual visual environments under different support base conditions. Experimental Brain Research. 2005; 167(4):535–556.

Mirka A, Black FO. Clinical application of dynamic posturography for evaluating sensory integration and vestibular dysfunction. Neurologic Clinics. 1990; 8(2):351–359. [PubMed: 2193216]

Miyamoto T, Fukushima K, Takada T, de Waele C, Vidal PP. Saccular stimulation of the human cortex: A functional magnetic resonance imaging study. Neuroscience Letters. 2007; 423(1):68–72. [PubMed: 17662530]

O'Connor KW, Loughlin PJ, Redfern MS, Sparto PJ. Postural adaptations to repeated optic flow stimulation in older adults. Gait & Posture. 2008; 28(3):385–391. [PubMed: 18329878]

Ohlendorf S, Sprenger A, Speck O, Haller S, Kimmig H. Optic flow stimuli in and near the visual field centre: A group fMRI study of motion sensitive regions. PLoS ONE. 2008; 3(12):e4043. [PubMed: 19112507]

Oliveira FTP, McDonald JJ, Goodman D. Performance monitoring in the anterior cingulate is not all error related: Expectancy deviation and the representation of action-outcome associations. Journal of Cognitive Neuroscience. 2007; 19(12):1994–2004. [PubMed: 17892382]

Palmisano S, Pinniger GJ, Ash A, Steele JR. Effects of simulated viewpoint jitter on visually induced postural sway. Perception. 2009; 38(3):442–453. [PubMed: 19485137]

Pietrini, P.; Ptito, M.; Kupers, R. Blindness and consciousness: New light from the dark. In: Laureys, S.; Tononi, G., editors. The Neurology of Consciousness. 1st. Academic Press; 2009. p. 360-374.

Poirier C, De Volder AG, Scheiber C. What neuroimaging tells us about sensory substitution. Neuroscience and Biobehavioral Reviews. 2007; 31(7):1064–1070. [PubMed: 17688948]

Ptito M, Moesgaard SM, Gjedde A, Kupers R. Cross-modal plasticity revealed by electrotactile stimulation of the tongue in the congenitally blind. Brain. 2005; 128(3):606. [PubMed: 15634727]

Redfern MS, Furman JM. Postural sway of patients with vestibular disorders during optic flow. Journal of Vestibular Research : Equilibrium & Orientation. 1994; 4(3):221–230.

Ricciardi E, Vanello N, Sani L, Gentili C, Scilingo EP, Landini L, Guazzelli M, Bicchi A, Haxby JV, Pietrini P. The effect of visual experience on the development of functional architecture in hMT+ Cerebral Cortex (New York, NY:1991). 2007; 17(12):2933–2939.

Robinson BS, Cook JL, Richburg CMC, Price SE. Use of an electrotactile vestibular substitution system to facilitate balance and gait of an individual with gentamicin-induced bilateral vestibular hypofunction and bilateral transtibial amputation. Journal of Neurologic Physical Therapy. 2009; 33(3):150–159. [PubMed: 19809394]

Rosner, B. Fundamentals of biostatistics. Thomson Brooks/Cole; Belmont, CA: 2006.

Satoh Y, Ishizuka KI, Murakami T. Modulation of the masseteric monosynaptic reflex by stimulation of the vestibular nuclear complex in rats. Neuroscience Letters. 2009; 466(1):16–20. [PubMed: 19781598]

Slobounov S, Wu T, Hallett M, Shibasaki H, Slobounov E, Newell K. Neural underpinning of postural responses to visual field motion. Biological Psychology. 2006; 72(2):188–197. [PubMed: 16338048]

Tracey I, Iannetti GD. Brainstem functional imaging in humans. Supplements to Clinical Neurophysiology. 2006; 58:52–67. [PubMed: 16623322]

Tyler M, Danilov Y, Bach-Y-Rita P. Closing an open-loop control system: Vestibular substitution through the tongue. Journal of Integrative Neuroscience. 2003; 2(2):159–164. [PubMed: 15011268]

Visser JE, Carpenter MG, van der Kooij H, Bloem BR. The clinical utility of posturography. Clinical Neurophysiology : Official Journal of the International Federation of Clinical Neurophysiology. 2008; 119(11):2424–2436. [PubMed: 18789756]

Vuillerme N, Cuisinier R. Sensory supplementation through tongue electrotactile stimulation to preserve head stabilization in space in the absence of vision. Investigative Ophthalmology & Visual Science. 2009; 50(1):476–481. [PubMed: 18708618]

Vuillerme N, Pinsault N, Fleury A, Chenu O, Demongeot J, Payan Y, Pavan P. Effectiveness of an electro-tactile vestibular substitution system in improving upright postural control in unilateral vestibular-defective patients. Gait & Posture. 2008; 28(4):711–715. [PubMed: 18632272]

Wall JT, Symonds LL, Kaas JH. Cortical and subcortical projections of the middle temporal area (MT) and adjacent cortex in galagos. The Journal of Comparative Neurology. 1982; 211(2):193–214. [PubMed: 7174890]

Weibull A, Gustavsson H, Mattsson S, Svensson J. Investigation of spatial resolution, partial volume effects and smoothing in functional MRI using artificial 3D time series. NeuroImage. 2008; 41(2): 346–353. [PubMed: 18400520]

Wildenberg JC, Tyler ME, Danilov YP, Kaczmarek KA, Meyerand ME. Sustained cortical and subcortical neuromodulation induced by electrical tongue stimulation. Brain Imaging and Behavior. 2010; 4(3-4):199–211. [PubMed: 20614202]
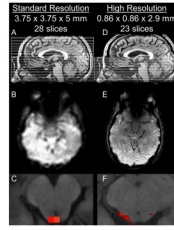
Figure 1.
A comparison of standard-resolution (A-C) and high-resolution functional MR imaging (D-F). A,D) Slice locations. B,E) Raw T2*-BOLD images. C,F) Single-subject activation of the superior colliculus in response to optic flow. The large voxels of the standard-resolution image are larger than the nuclei themselves. The voxels of the high-resolution image are much smaller than individual nuclei.
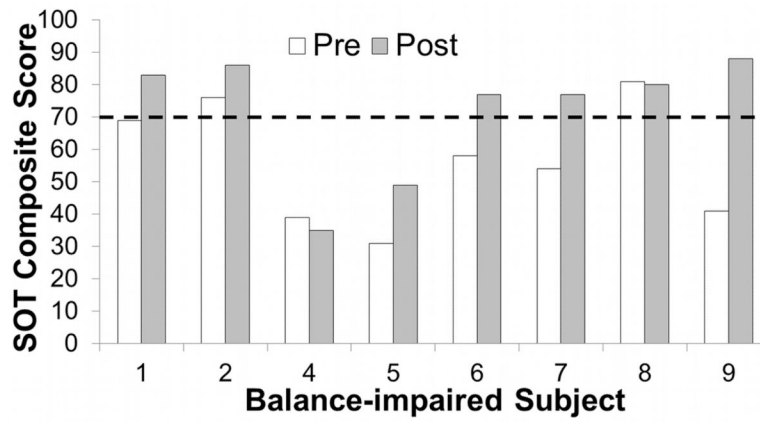
Figure 2.
Scores from the sensory organization tests (SOTs) before and after CN-NINM stimulation. The dashed line shows the cutoff for impairment as defined by the test. One subject was not able to complete the pre-stimulation testing and is therefore not included. Pre – balance subjects before stimulation. Post – balance-impaired subjects after stimulation.
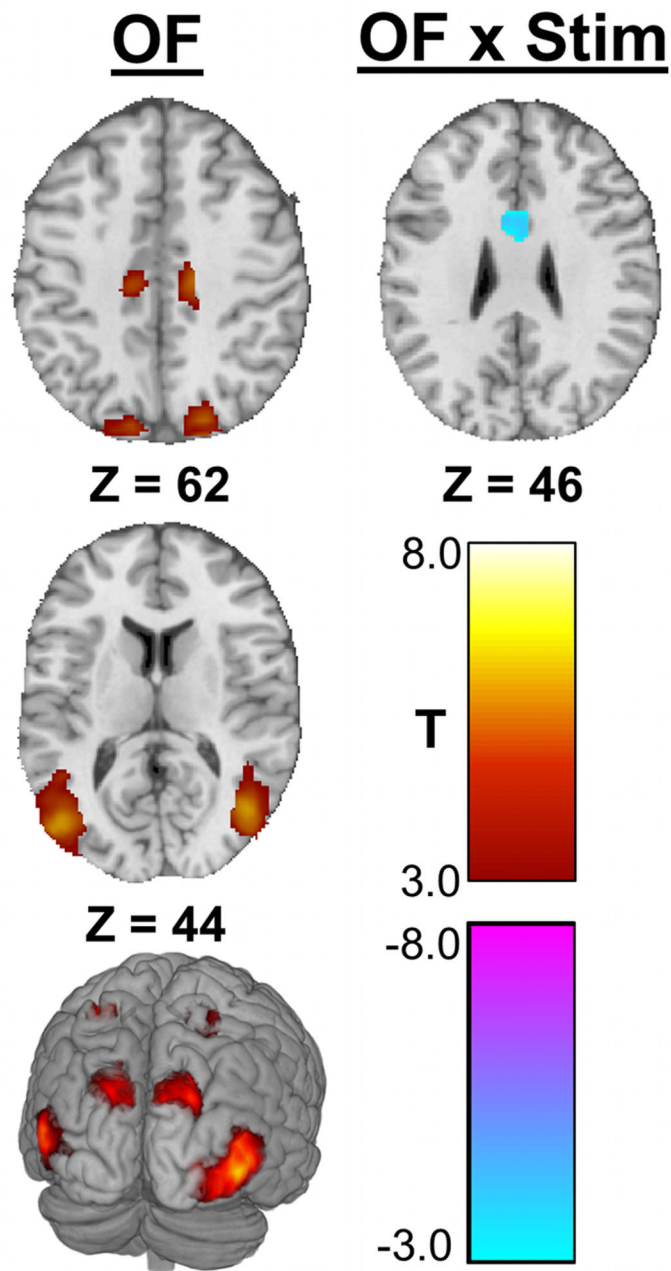
Figure 3.
Significant clusters in the stan-res data from the two-way ANOVA. This analysis compared balance-impaired subjects before stimulation (Pre) to after stimulation (Post). OF shows activity attributable to the effects of optic flow while OF × Stim indicates regions where optic flow-related processing changed after stimulation. No clusters reached significance for the effect of stimulation alone (Stim). Images are thresholded at $\alpha \leq 0.005$. Only clusters with a volume greater than 1144 µl are displayed. All Z values are in MNI coordinates.
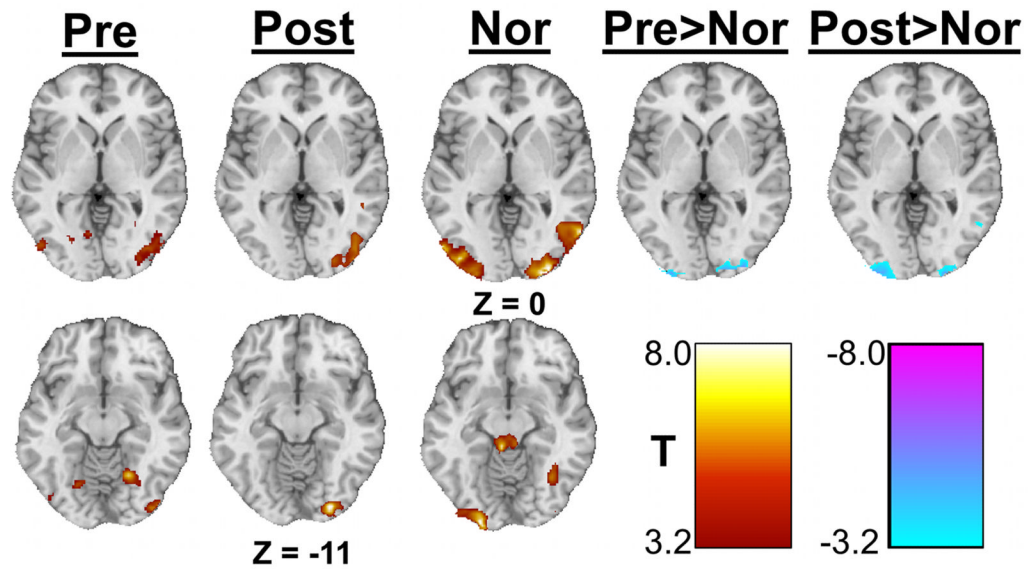
Figure 4.
Significant clusters from the one- and two-sample *t*-tests showing the effect of optic flow. The first three columns show activity due to optic flow in each group separately while the last two columns show intergroup comparisons (Pre>Nor shows differences between balance-impaired subjects before stimulation to healthy controls, Post>Nor shows differences between balance-impaired subjects after stimulation to healthy controls). Images are thresholded at $\alpha \leq 0.005$. Only clusters with a volume greater than 1144 µl are displayed. All Z values are in MNI coordinates.
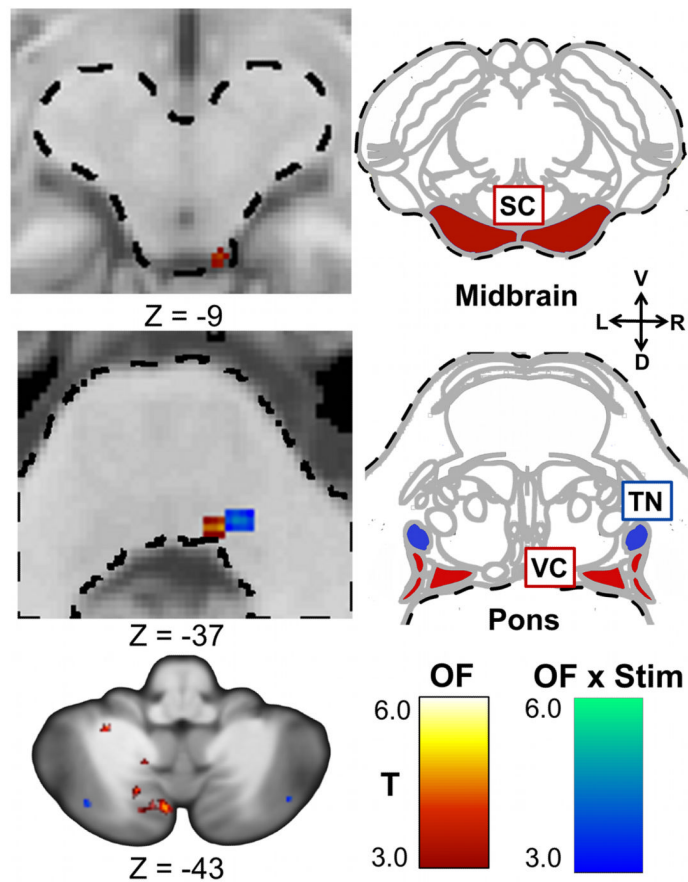
Figure 5.
Significant clusters within the brainstem and cerebellum from the high-res data in the two-way ANOVA. This analysis compared balance-impaired subjects before stimulation (Pre) to after stimulation (Post). OF shows activity attributable to the effects of optic flow while OF × Stim indicates regions where optic flow-related processing changed after stimulation. No clusters reached significance for the effect of stimulation alone (Stim). In the top two rows, the left column shows significant clusters while the right column shows axial diagrams of the brainstem at the approximate axial location (Duvernoy 1995). The image in the lower left shows significant clusters within the cerebellum. The labeled structures in the diagrams are the most likely nuclei of the activation clusters. Images are thresholded at $\alpha \leq 0.005$. Only clusters with a volume greater than 20 μl are displayed. All Z values are in MNI coordinates. The dashed line outlines the brainstem. (Abbreviations: TN, trigeminal nucleus; VC, vestibular nuclei complex; R/L/V/D, right/left/ventral/dorsal)

Table 1

Locations and volumes of the activation clusters from the two-way ANOVA of the stan-res data. Optic flow activated several regions known to be involved in processing visual-motion including the visual association cortices. This analysis compared balance-impaired subjects before stimulation (Pre) to after stimulation (Post). OF shows activity attributable to the effects of optic flow while OF × Stim indicates regions where optic flow-related processing changed after stimulation. No clusters reached significance for the effect of stimulation alone (Stim) therefore that column is omitted. Only clusters with volume greater than 1144 microliters are included. Coordinates are the center of mass in MNI space. (Abbreviations: CSv: Cingulate sulcus visual area; R/L/M: right/left/midline, #: decreased activation)

| Region | R/L | OF | | OF × Stim | |
		Coordinates	Vol.	Coordinates	Vol.
Standard Resolution					
Lateral Occipital Gyrus	R	(40,−71,5)	24,696		
	L	(−45,−72,7)	17,352		
Superior Parietal Lobule	R	(22,−84,35)	6,720		
	L	(−15,−85,35)	6,700		
Post-Central Gyrus	R	(22,−52,63)	3,472		
	L	(−27,−53,62)	4,296		
CSv	R	(13,−22,44)	1,960		
	L	(−10,−22,44)	1,824		
Facial Gyrus	R	(21,−62,−9)	2,200		
	L	(−19,−69,−6)	1,856		
Anterior Cingulate	M			(2,8,30)#	1,800

Table 2

Locations and volumes of the activation clusters from one- and two-sample *t*-tests of the stan-res data. In each group, optic flow activated several visual association cortices. Normal controls had greater activity of V1 than the balance subjects both before and after stimulation. The first three columns show activity due to optic flow in each group separately while the last two columns show intergroup comparisons (Pre>Nor shows differences between balance-impaired subjects before stimulation to healthy controls, Post>Nor shows differences between balance-impaired subjects after stimulation to healthy controls). Only clusters with volume greater than 1144 microliters are included. Coordinates are the center of mass in MNI space. (Abbreviations: L, lateral; S/I, superior/inferior; SPL, superior parietal lobule; R/L/B, right/left/bilateral; #, decreased activation)

Region	R/L	Pre		Post		Nor		Pre>Nor		Post>Nor	
		Coordinates	Vol.	Coordinates	Vol.	Coordinates	Vol.	Coordinates	Vol.	Coordinates	Vol.
Standard Resolution											
L. Occipital Gyrus	R	(42,-78,1)	7,936	(37,-83,-5)	5,960	(48,-64,0)	8,072				
	L	(-46,-75,1)	3,000			(-46,-76,6)	11,570				
SPL	R	(24,-88,34)	8,848	(19,-83,39)	1,880	(22,-75,38)	2,728				
	L	(-10,-88,34)	9,936								
Post-Central Gyrus	L	(-26,-58,64)	1,504	(-27,-54,64)	1,208						
Angular Gyrus	R			(51,-42,6)	1,224	(60,-38,19)	1,192				
Facial Gyrus	R	(26,-61,-14)	3,520								
	L	(-19,-67,-10)	2,704								
Cuneus	R					(28,-93,-1)	6,088	(25,-94,2)#	1,528	(25,-98,4)#	1,504
	L					(-30,-91,-3)	4,958	(-22,-99,1)#	1,248	(-24,-98,0)#	2,424
Superior Colliculus	B					(-1,-35,-16)	3,904				
I. Semilunar Lobule	B					(5,-62,-45)	5,416				

Table 3

Locations and volumes of the activation clusters from the two-way ANOVA of the high-res data. Optic flow activated the superior colliculus and the vestibular nuclei as well as several regions in the cerebellum. The trigeminal nucleus showed increased activity in response to optic flow after stimulation compared to before. This analysis compared balance-impaired subjects before stimulation (Pre) to after stimulation (Post). OF shows activity attributable to the effects of optic flow while OF × Stim indicates regions where optic flow-related processing changed after stimulation. No clusters reached significance for the effect of stimulation alone (Stim) therefore that column is omitted. Only clusters with a volume greater than 20 microliters are included. Coordinates are the center of mass in MNI space. (Abbreviations: S/I, superior/inferior; R/L/M, right/left/midline, #, decreased activation)

Region	R/L	OF Coordinates	Vol.	OF × Stim Coordinates	Vol.
High Resolution					
Trigeminal Nucleus	R			(12,-34,-38)	62
Vestibular Complex	R	(9,-35,-37)	20		
Superior Colliculus	R	(10,-34,-13)	106		
Pontine White Matter	R			(2,-31,-32)	20
	L			(-2,-21,-30)	32
Medial Lemniscus	L	(-9,-32,-27)	20		
Central Lobule	R			(9,-49,-18)	20
S. Semilunar Lobule	R			(48,-70,-39)	20
	L			(-41,-67,-39)	34
Quadrangular Lobe	L			(-21,-66,-28)	26
	R	(30,-59,-24)	38		
	L			(-19,-60,-28)#	24
Declive	M	(1,-72,-28)	52		
Deep Cerebellar Nuclei	R			(9,-56,-28)	36
Pyramid of Vermis	L	(-6,-68,-36)	78		
I. Semilunar Loblue	R			(40,-72,-47)	74
	L	(-16,-69,-45)	58	(-23,-76,-47)	64
	L	(-7,-81,-47)	34	(-34,-73,-42)	88
	L	(-17,-76,-50)	24	(-35,-69,-48)	28
	L	(-7,-76,-40)	336		
Biventer Lobe	L	(-13,-60,-46)	40		
	L	(-27,-47,-43)	38		

Table 4

Locations and volumes of the activation clusters from one- and two-sample *t*-tests of the high-res data. The large number of activation clusters detected by this analysis likely reflects greater consistency in subcortical activation in the normal group compared to the balance subjects. The first three columns show activity due to optic flow in each group separately while the last column shows differences between balance-impaired subjects after stimulation to healthy controls (Post>Nor). The comparison of balance-impaired subjects before CN-NINM (Pre) to healthy controls (Nor) did not produce any significant activation clusters therefore that column is omitted. Only clusters with volume greater than 20 microliters are included. Coordinates are the center of mass in MNI space. (Abbreviations: S/I, superior/inferior; R/L/M, right/left/midline, #, decreased activation)

Region	R/L	Pre Coordinates	Pre Vol. (µl)	Post Coordinates	Post Vol. (µl)	Nor Coordinates	Nor Vol. (µl)	Post>Nor Coordinates	Post>Nor Vol. (µl)
High Resolution									
Superior Colliculus	R					(9,-36,-6)	92		
	L					(-6,-34,6)	34		
Quadrangular Lobe	R					(11,-71,-19)	94		
	L					(-5,-73,-19)	130		
	L					(-24,-66,-20)	28		
Simple Lobule	R					(33,-54,-30)	28		
	R					(14,-67,-27)	26		
	R					(14,-64,-26)	24		
Nodulus	M					(2,-59,-35)	42	(3,-60,-35#)	22
Culmen	M					(3,-70,-31)	146		
S. Semilunar Lobule	L							(-35,-69,-41)	34
I. Semilunar Lobule	L	(-6,-73,-43)	26			(-5,-73,-40)	208		
Pyramid of Vermis	M					(-2,-63,-43)	24		
Tonsil	R					(6,-56,-43)	24		
Uvula	M					(2,-51,-43)	20		
Dentate Nucleus	L	(-12,-57,-35#)	22						
Biventer Lobe	R					(14,-54,-49)	40		
	L			(-18,-56,-47)	22	(-12,-60,-53)	92		